

Study of the $\text{Ne}(^3P_2) + \text{CH}_3\text{F}$ Electron Transfer Reaction below 1 Kelvin

Justin Jankunas, Benjamin Bertsche, and Andreas Osterwalder*

*Institute for Chemical Sciences and Engineering, Ecole Polytechnique Fédérale de Lausanne,
1015 Lausanne, Switzerland*

E-mail: andreas.osterwalder@epfl.ch

*To whom correspondence should be addressed

Abstract

Relatively little is known about the dynamics of electron transfer reactions at low collision energy. We present a study of Penning ionization of ground state methyl fluoride molecules by electronically excited neon atoms in the 13 μeV –4.8 meV (150 mK–56 K) collision energy range, using a neutral-neutral merged beam setup. Relative cross sections have been measured for three $\text{Ne}(^3P_2) + \text{CH}_3\text{F}$ reaction channels by counting the number of CH_3F^+ , CH_2F^+ , and CH_3^+ product ions, as a function of relative velocity between the neon and methyl fluoride molecular beams. Experimental cross sections markedly deviate from the Langevin capture model at collision energies above 20 K. The branching ratios are constant. In other words, the chemical shape of the CH_3F molecule, as seen by $\text{Ne}(^3P_2)$ atom, appears not to change as the collision energy is varied, in contrast to related $\text{Ne}(^3P_J) + \text{CH}_3\text{X}$ ($\text{X}=\text{Cl}$ and Br) reactions at higher collision energies.

Introduction

The experimental and theoretical study of electron transfer reactions addresses one of the most fundamental processes in chemistry and biology. Such reactions occupy a special place in the world of gas phase reaction dynamics because they were among the first reactions that were studied during the first phase of molecular beam based studies of reaction dynamics.¹ Penning ionization (PI), commonly described as $\text{A}^* + \text{B} \rightarrow \text{A} + \text{B}^+ + \text{e}^-$, can be viewed as an electron transfer reaction wherein the internal energy of one reactant, A^* , is greater than the ionization potential of the other, B. The reaction proceeds by an electron transfer from target molecule B into one of the empty orbitals of A^* , leading to ejection of the least tightly bound electron in species A. A great deal of experimental measurements and theoretical calculations have been performed on simple PI systems,² most notably atom-atom and atom-diatom reactions. They suggest that electronic orbital overlap between the reactants determines the internal state population distribution of the B^+ product ion, as well as the Penning electron kinetic energy spectrum.³ A particularly interesting case of PI is when B is a small polyatomic molecule. Then, the presence of several (non-degenerate)

molecular orbitals means that the potential energy, associated with a particular geometry of the $[AB]^*$ complex, can vary for different A–B approach directions. Ionization from different molecular orbitals produces different states of the molecular cation, dictated by correlation rules between the electronic states of neutral and ionized molecular species. Since the shape of the molecular orbitals is directly linked to the structure of the molecule, the measurement of branching ratios can serve as a stereodynamic probe of a particular PI reaction.

Several Penning ionization studies of small polyatomic molecules by electronically excited helium and neon atoms have been performed to date. For example, Vecchiocattivi and co-workers examined $Ne(^3P_J) + H_2O$ PI in the range of collision energies E_{coll} 40 meV–300 meV (465 K–3480 K; here, temperature is defined as $T = E_{coll}/k_B$).^{4–6} The internal $Ne(^3P_J)$ energy of ≈ 16.7 eV made accessible two channels, correlating asymptotically with a molecular water cation in the ground and electronically excited states, $H_2O^+(X^2B_1)$, and $H_2O^+(A^2A_1)$, respectively. The reaction cross section was found to increase with decreasing collision energy, suggesting an attractive nature of $Ne(^3P_J) - H_2O$ collisions in the E_{coll} range studied. The relative yield of electronically excited products increased modestly with decreasing collision energy. Similar branching ratio behavior has been observed in the PI of N_2O by He^* and Ne^* .⁷ On the other hand, the fraction of electronically excited NH_3^+ product ions decreases modestly with decreasing E_{coll} , as found in the study of collisions between $Ne(^3P_J)$ atoms and NH_3 in the range of E_{coll} 35 meV–200 meV (406 K–2320 K).⁸ Penning ionization of methyl halides, CH_3X , is even more interesting, due to a larger number of open reactive channels. Photoionization studies of CH_3F have revealed five open channels at photon energies of 16.5–17 eV: production of CH_3F^+ , as well as dissociative channels producing CH_2F^+ , CH_3^+ , CHF^+ , and CH_2^+ .⁹ Cross sections for double dissociation have been measured to be at least 20 times smaller than the single dissociation cross sections which in turn were similar to non-dissociative photoionization. PI studies of methyl halides have shown the dissociative channels CH_3^+ , CH_2X^+ , and the non-dissociative channel CH_3X^+ . Brunetti et al.¹⁰ have investigated the $Ne(^3P_J) + CH_3X$ ($X=Cl$ and Br) reactions and reported an increasing fraction of parent ions with decreasing collision energy, whereas the fragment yield decreased

with diminishing E_{coll} . The general assumption in the interpretation of these experiments was that the propensities to form ions in the different electronic states is related to the orientation of the molecule relative to the angle of incidence of the metastable atom. In the case of $\text{NH}_3 + \text{Ne}(^2P_J)$, for example, the ionic ground state is formed by removing an electron from the nitrogen lone pair while the first excited state is formed by removing an electron from one of the N-H bond orbitals.⁸ In PI, accordingly, ground state NH_3^+ is formed when the Ne^* approaches along the N-lone pair axis while electronically excited $\text{NH}_3^+(\text{A})$ is formed when the Ne^* approaches along an N-H bond. If the ground state cation is stable to dissociation but the excited state is not, then mass selective detection of the product ions is a direct measure of the branching ratio during the PI and thus a probe for the stereo dynamics of the reaction. In those cases where the ionic states formed upon electron transfer can dissociate along different routes and form the same products one can make use of the fact that the internal branching ratios, i.e. those that determine the fate of ions formed in particular states, are independent of the collision energy. Any dependence of the measured branching ratios on E_{coll} can thus be attributed to the stereo dynamics of the electron transfer process itself. All of the PI experiments mentioned above have been carried out at collision energies close to and above $E_{\text{coll}}/k_B = 300 \text{ K}$ (25 meV). We report on an experimental study of $\text{Ne}(^3P_2) + \text{CH}_3\text{F}$ PI in the 13 μeV – 4.8 meV (150 mK–56 K) collision energy range. The present study represents the first investigation of PI of a six-atom reaction system in this energy range. To this date, the largest molecule studied below 10 meV was ammonia.^{11–13} Unlike the Penning fragment branching ratios that exhibit a noticeable dependance on E_{coll} above 300 K, we find that the relative yield of three reaction channels CH_3F^+ , CH_2F^+ , and CH_3^+ is, within the experimental uncertainty, constant in the E_{coll} range studied. This observation is surprising: a straightforward argument based on the well depth for different $[\text{Ne}-\text{CH}_3\text{F}]^*$ configurations, as was successfully applied in the case of $\text{Ne}(^3P_J) + \text{H}_2\text{O}$ reaction at higher collision energies,⁴ predicts a particular reaction channel to become dominant with ever decreasing collision energy.

Experimental

The low collision energy of $13\text{ }\mu\text{eV}$ was achieved in a neutral-neutral merged beam technique.^{11–15} The experimental apparatus is described elsewhere.^{12,13} Briefly, a supersonic beam of neon atoms in the excited $\text{Ne}(2p^5\ 3s^1,\ ^3P_2)$ state is bent by means of a magnetic hexapole guide, and merged with a molecular beam of electrostatically guided CH_3F molecules in the electronic ground state.^{16–18} Only the $J = 2$ spin-orbit component of the $2p^5\ 3s^1\ ^3P_J$ state of neon is present in the reaction since the $J = 1$ component is short-lived and the $J = 0$ component is not paramagnetic. The rotational state distribution of CH_3F molecules is broader and harder to quantify than the single-state Ne beam. Based on resonance enhanced multiphoton ionization (REMPI) spectra of ND_3 molecules that are co-expanded and guided together with the desired CH_3F molecules we estimate the rotational temperature to be $\approx 20\text{ K}$. Because of the rotational state dependent guiding dynamics the rotational degrees of freedom are not in thermal equilibrium.¹⁸ Calculating the CH_3F (J, K) state populations present in the interaction region is challenging. Based on our earlier finding wherein ND_3 molecules before entering and after exiting the molecular guide exhibited different rotational temperatures,¹⁸ we must assume that rotational distributions of CH_3F molecules before and after entering the electric field region are also different. Assuming $T_{\text{rot}} = 20\text{ K}$ for CH_3F molecules immediately following the supersonic expansion, then over 95% of molecules reside in $J \leq 5$ levels. More importantly, over 60% of CH_3F molecules occupy the $K = 0$ state, whilst the remaining $\approx 40\%$ fraction of molecules are in $3 \leq K \leq 1$ states. Methyl fluoride molecules in $J \geq 1, K = 0$ rotational levels exhibit only a quadratic Stark effect, and are therefore expected to be guided less efficiently than the $K \geq 1$ states whose energy is linearly proportional to the electric field strength inside the hexapole guide.

The crossing angle between the two merged molecular beams is zero, and the average relative velocity between reactants v_{rel} is zero when the laboratory speeds of $\text{Ne}(^3P_2)$ and CH_3F beams are the same. As explained previously,^{11,13,19} the resolution in E_{coll} is dictated mainly by a finite duration of the molecular beam pulse. In the present case the velocity spread at each relative velocity is $\approx 28\text{ m/s}$. The lowest attainable collision energy is half of that because with both

beams centred around the same velocity the average relative velocity is $\langle v_{rel} \rangle = 0 \pm 28$ m/s, and $\langle |v_{rel}| \rangle = 14 \pm 14$ m/s, assuming a square distribution of the velocities. The spread of collision energies scales quadratically with the average velocity, and the minimum central velocity we can reach corresponds to an average collision energy $E_{coll,min}/k_B = 120$ mK. Transverse velocities in the present experiment contribute to the spread in collision energy to a lesser amount and are neglected.¹³ Fragment ions are collected in a time-of-flight mass spectrometer and counted mass-selectively. The number of collected ions is proportional to the absolute reaction cross section and the beam-densities and -overlap; due to the difficulties to quantify the latter two, no absolute cross sections can be reported.

Results and Discussion

Measured reaction cross sections are shown in 1A. Cross sections for CH_3^+ (red squares), CH_2F^+ (black triangles), and CH_3F^+ (green rhombs) product formation are shown individually, and the sum is plotted as blue circles, showing the total $\text{Ne}(^3P_2) + \text{CH}_3\text{F}$ PI probability. The grey curve is the Langevin capture (LC) model prediction for an intermolecular potential $V(R) \propto R^{-6}$, where the cross section $\sigma \propto E_{coll}^{-1/3}$. The LC model predicts σ to decrease with increasing collision energy. A log-log plot of σ vs. E_{coll} yields a straight line with a slope of $-1/3$.³ The $\text{Ne}(^3P_2) + \text{CH}_3\text{F}$ molecular collisions are dominated by long range interactions proportional to $V(R) \propto R^{-6}$ up to about 20 K. At $E_{coll} > 20$ K the data start to deviate from the LC model, suggesting that other potential energy terms begin to contribute.

We now turn to the measured branching ratios. Experimental results, defined as

$$\Gamma(i) = \frac{[i]}{[\text{CH}_3^+] + [\text{CH}_2\text{F}^+] + [\text{CH}_3\text{F}^+]}, \quad (1)$$

for the three reaction channels are shown in 1B.

In order to disentangle the different reaction channels that can lead to the observed branching ratios we refer to the diagram in 2. The left side shows the initial level of the combined

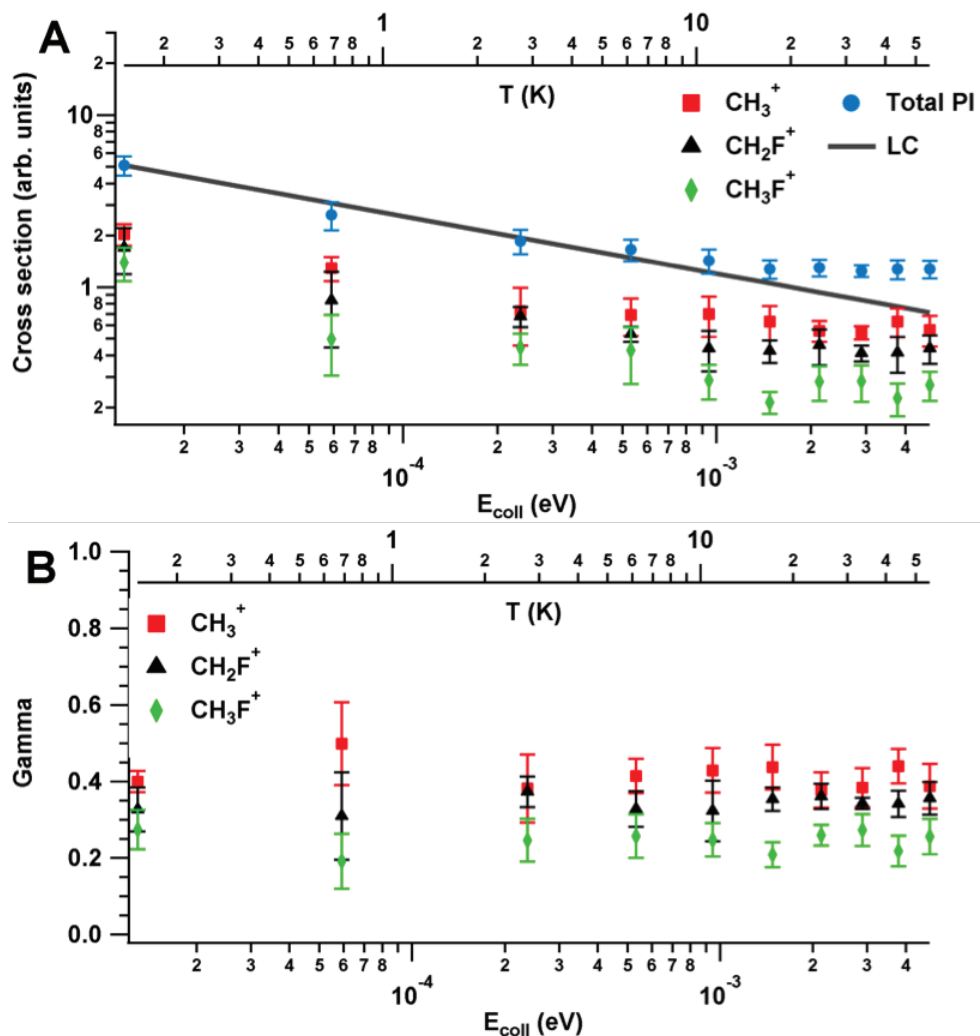


Figure 1: (A) Partial and total $\text{Ne}(^3P_2) + \text{CH}_3\text{F}$ Penning ionization cross sections. Red squares: CH_3^+ products; black triangles: CH_2F^+ products; green rhombs: CH_3F^+ products; blue circles: total PI cross section ($\text{CH}_3^+ + \text{CH}_2\text{F}^+ + \text{CH}_3\text{F}^+$). The solid grey curve shows the prediction based on the Langevin capture model. (B) Branching ratios, $\Gamma(i)$, for the three reactive channels as a function of collision energy. Color coding is the same as in panel (A).

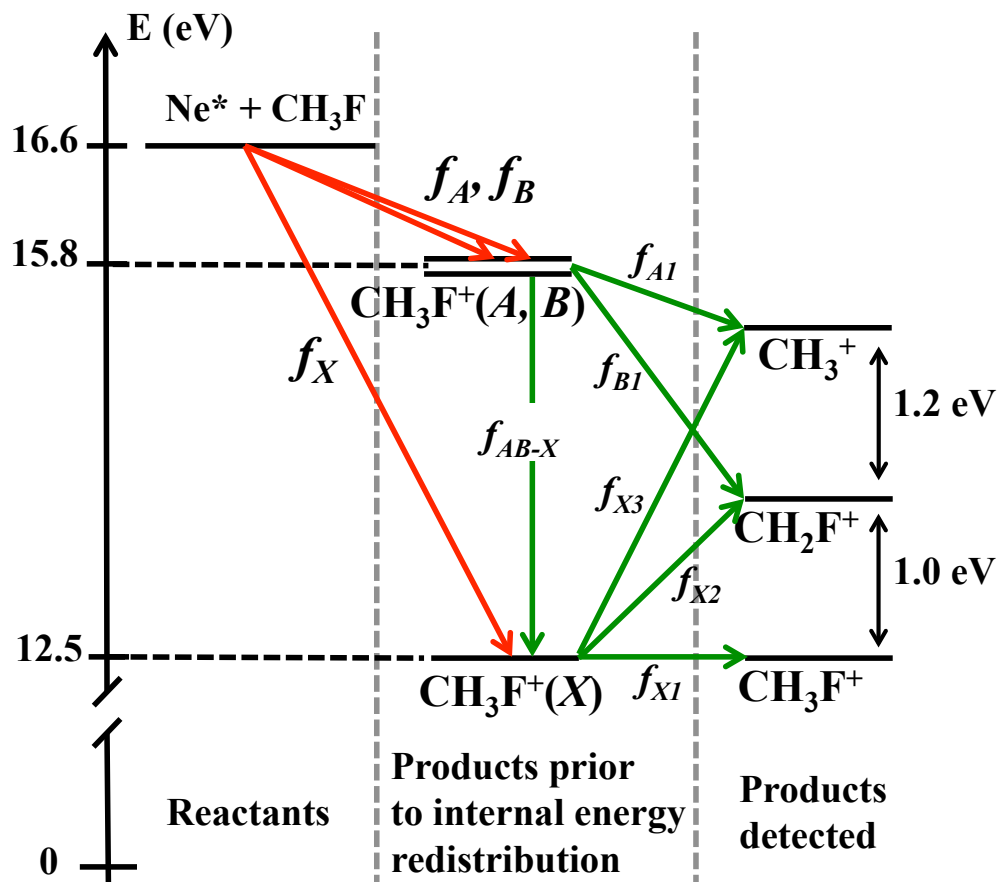


Figure 2: Energy diagram for the $\text{Ne}(^3P_2) + \text{CH}_3\text{F}$ reaction, illustrating the three accessible electronic states of CH_3F^+ product cation, with the associated collision induced and internal conversion/dissociation branching ratios indicated by red and green arrows, respectively.

Ne(3P_2)+CH₃F system at the internal energy of Ne(3P_2). PI can lead to the formation of CH₃F⁺ ions in the X, A, or B state, as shown in the central part. These states can decay into the observed fragments on the right side of 2. The experimentally observed branching ratios are a convolution of the desired branching ratios f_X , f_A , and f_B and the internal branching ratios, labeled as f_{X1} , f_{X2} , f_{X3} , f_{AB-X} , f_{A1} , and f_{B1} , which are not known. The excited A and B states have short life times such that it can be assumed that all excited ions will decay by one of the pathways indicated in the figure. The branching ratios are related by an underdetermined set of equations. However, limits can be set on f_X that allow to shed some light on the observed dynamics. It is known that CH₃X⁺ cations (X = F, Cl, Br, I) in several electronically excited states are subject to various internal conversion, conical intersection, and dissociative processes.²⁰ However, it has been observed that in CH₃F⁺ the only decay channel for the A and B states is the formation of CH₃⁺.²¹ This implicitly means that f_{AB-X} and f_{B1} are all zero. The latter can be rationalised by the coupling of the A- and B-states. Unlike in CH₃Cl⁺, CH₃Br⁺, and CH₃I⁺ molecules, the excited A- and B-states of the CH₃F⁺ cation are degenerate. This makes the following analysis easier, because the internal conversion (IC) from B to A is often said to proceed with a 100% efficiency.²¹ Assuming IC from B to A to be much faster than the molecular dissociation CH₃F⁺(B) → CH₂F⁺ + H (see 2), the resulting equations can be solved to put limits on the f_X , f_A , and f_B values. $f_{AB-X} \neq 0$ would potentially open a path to CH₃F⁺ formation via PI to one of the excited states. Branching ratios for the formation of [CH₃⁺], [CH₂F⁺], and [CH₃F⁺] are defined by equation 1. The detailed balance dictates the following relations between these and the individual branching ratios f_X , f_A , f_B , and f_{X1} , f_{X2} , f_{X3} , f_{A1} , f_{B1} (see 2):

$$\begin{aligned}
 \Gamma(\text{CH}_3^+) &= f_X f_{X3} + f_A f_{A1} \\
 \Gamma(\text{CH}_2\text{F}^+) &= f_X f_{X2} + f_B f_{B1} \\
 \Gamma(\text{CH}_3\text{F}^+) &= f_X f_{X1} \\
 f_X + f_A + f_B &= 1 \\
 f_{X1} + f_{X2} + f_{X3} &= 1
 \end{aligned}$$

$$f_{A1} + f_{B1} = 1.$$

The assumption that the IC is much faster than the corresponding $\text{CH}_3\text{F}^+(\text{B}) \rightarrow \text{CH}_2\text{F}^+ + \text{H}$ dissociation, allows the above equations to be simplified because $f_{B1} = 0$. Furthermore, f_{AB-X} has been observed to be zero²¹ by the lack of CH_3F^+ formation via the excited A- or B-states. Making use of the fact that all $\Gamma[i]$ are, within the experimental uncertainty, insensitive to the collision energy we can average the branching ratios over the entire collision energy range studied to obtain $\Gamma(\text{CH}_3^+) = 0.42 \pm 0.04$, $\Gamma(\text{CH}_2\text{F}^+) = 0.34 \pm 0.02$, and $\Gamma(\text{CH}_3\text{F}^+) = 0.24 \pm 0.03$. Limits on f_X are then given as $0.58 < f_X < 1.00$ by assuming either $f_A \cdot f_{A1} = 0$, in which case $f_X = 1$, or by assuming $f_{X3} = 0$ in which case $f_X = \Gamma(\text{CH}_3\text{F}^+) + \Gamma(\text{CH}_2\text{F}^+) = 0.58$ and $f_A + f_B = 0.42$. In the limit $f_X = 1$ we have, by definition, $f_B = f_A = 0$. The resulting $\text{CH}_3\text{F}^+(\text{X})$ cation dissociates into experimentally detected CH_3F^+ , CH_2F^+ , and CH_3^+ products with branching ratios of $f_{X1} = 0.24$, $f_{X2} = 0.34$, and $f_{X3} = 0.42$, respectively. Conversely, if $f_X = 0.58$, then 42% of all $\text{Ne}(^3P_2) + \text{CH}_3\text{F}$ collisions populate the degenerate A and B electronic states which, assuming fast IC (*vide supra*), dissociate completely into CH_3^+ products. In this scenario the $\text{CH}_3\text{F}^+(\text{X})$ products branch out into the detected CH_3F^+ and CH_2F^+ ions with $f_{X1} = 0.41$, and $f_{X2} = 0.59$, respectively, whilst $f_{X3} = 0$.

Given the energetics of the reaction it is safe to assume the f_{X1} , f_{X2} , f_{X3} , f_{A1} , and f_{B1} to be independent of collision energy. Consequently, also the f_X , f_A , and f_B remain constant as the collision energy increases from 150 mK up to 56 K which in view of previous observations at higher E_{coll} is surprising. It is tempting to attribute this finding solely to the fact that the current experiment was performed at low collision energies, whereas previous branching ratios that did depend on E_{coll} , were measured at $E_{\text{coll}} > 25$ meV (300 K). The increasing fraction of CH_2X^+ ($X = \text{Cl}, \text{Br}$) and CH_3^+ Penning fragments with growing collision energy has been explained by drawing attention to different potential energy slopes for $\text{Ne}(^3P_J)$ approach toward the -X and - CH_3 end of the CH_3X molecule.¹⁰ They suggest that the softer repulsive potential around the methyl group results in a greater fragmentation at higher E_{coll} . While it is hard to rule out the above argument based on the current findings at $E_{\text{coll}} \ll 300$ K, one would expect a particular reaction

channel, in this case $\text{Ne}(^3P_J)$ approach from either side along the C-F axis of CH_3F , to be ever more favored as $E_{\text{coll}} \rightarrow 0$ eV. This is not what is observed experimentally. One way to understand the constant yield of the three reaction products as a function of collision energy is to consider the $f_X = 1$ scenario: all reactive $\text{Ne}(^3P_2) + \text{CH}_3\text{F}$ collisions populate only the ground electronic state of $\text{CH}_3\text{F}^+(\text{X})$ ion which then dissociates into the detected products with the branching ratios f_{X1} , f_{X2} , and f_{X3} . This hypothesis is disfavored by the experiments wherein Penning electrons, as opposed to fragment ions, have been detected. Methyl fluoride molecules, ionized with He I and Ne I radiation, yielded electrons with a bimodal kinetic energy distribution, corresponding to the production of $\text{CH}_3\text{F}^+(\text{X})$ and $\text{CH}_3\text{F}^+(\text{A}, \text{B})$ ions.²¹ A related $\text{Ne}(^3P_J) + \text{NH}_3$ system correlating with NH_3^+ and NH_2^+ product ions has been shown to proceed via $\text{NH}_3^+(\text{X})$ and $\text{NH}_3^+(\text{A})$ electronic states, respectively, as deduced from electron kinetic energy analysis.⁸ The exclusive formation of ground state $\text{CH}_3\text{F}^+(\text{X})$ product ions is therefore unlikely, although not impossible.

Conclusions

Study of electron transfer reactions at collision energies below 1 Kelvin ($85 \mu\text{eV}$) has only begun to unravel our limited understanding of low-energy molecular collisions. In addition to the observation of elusive shape resonances in the $\text{He}^* + \text{H}_2$ PI,^{14,15} chemical reactions at low temperatures exhibit rather unusual stereodynamics.²² The study of the $\text{Ne}(^3P_2) + \text{CH}_3\text{F}$ reaction in the low temperature regime has shown yet again energy independent branching ratios, similar to what has been observed in $\text{Ne}(^3P_2) + \text{ammonia}$.^{11–13} Similar Penning ionization studies carried out at collision energies close to and above room temperature have shown that branching ratios do depend on E_{coll} . In certain cases the ratio of dissociative PI increases with a growing collision energy,^{8,10} and at other times it does the opposite.^{4–7} We have not been able to conclusively establish the origin of the constant $\Gamma(i)$ values, and we are left to speculate: (a) The dynamics of $\text{Ne}(^3P_2) + \text{CH}_3\text{F}$ reaction at low temperatures changes drastically, and only the $\text{CH}_3\text{F}^+(\text{X})$ product ion in its ground electronic state is produced. This would be in sharp contrast to PI experiments at

higher energies, where several (energetically accessible) electronic states of the polyatomic cation are populated. (b) A more probable and, unfortunately, currently less insightful, scenario is the combination of the increased de Broglie wavelength, with the ratio of collision time to rotational period of CH_3F , which also increases with decreasing E_{coll} . Although a quantitative assessment of this effect at this point is not possible it is easily imagined that this also results in constant branching ratios. Fully dimensional $\text{Ne}(^3P_2) + \text{CH}_3\text{F}$ quantum calculations at the moment appear to be unaffordable, however classical or quasiclassical calculations could potentially shed some light on the question of constant branching ratios in $\text{Ne}(^3P_2) + \text{CH}_3\text{F}$ reaction. (c) Finally it must also be pointed out that our energy-dependent branching ratio expectations are based on high temperature reaction dynamics between reagents in the ground electronic states. Often such reactions have significant (chemical) reaction barriers. The height of the barrier depends on the direction of approach of the reactants - a realm of stereodynamics, which taught us the idea of a minimum energy path. Barrierless reactions, like $\text{Ne}(^3P_J) + \text{CH}_3\text{F}$, that occur at low collision energies have a unit opacity function at large internuclear separations.³ Theoretical calculations are once again needed to provide a full understanding by calculating, for example, the energy difference between several $[\text{Ne}-\text{CH}_3\text{F}]^*$ conformers at large internuclear separations.

Acknowledgement

We thank Rainer Beck and Marcel Drabbels (both EPFL) for lending us scientific equipment and the Swiss Science foundation (grant number P00P2-144924) and the EPFL for funding.

References

- (1) Levine, R. D. *Molecular Reaction Dynamics*; Cambridge University Press: Cambridge, 2009.
- (2) Siska, P. E. Molecular-beam studies of Penning ionization. *Rev. Mod. Phys.* **1993**, 65, 337–412.

- (3) Niehaus, A. Spontaneous Ionization in Slow Collisions. *Advances in Chemical Physics* **1981**, 45, 399–486.
- (4) Brunetti, B.; Candori, P.; Cappelletti, D.; Falcinelli, S.; Pirani, F.; Stranges, D.; Vecchiocattivi, F. Penning ionization electron spectroscopy of water molecules by metastable neon atoms. *Chem. Phys. Lett.* **2012**, 539, 19–23.
- (5) Balucani, N.; Bartocci, A.; Brunetti, B.; Candori, P.; Falcinelli, S.; Palazzetti, F.; Pirani, F.; Vecchiocattivi, F. Collisional autoionization dynamics of $\text{Ne}(^3\text{P}_{2,0})\text{-H}_2\text{O}$. *Chem. Phys. Lett.* **2012**, 546, 34–39.
- (6) Brunetti, G. B.; Candori, P.; Falcinelli, S.; Pirani, F.; Vecchiocattivi, F. The Stereodynamics of the Penning Ionization of Water by Metastable Neon Atoms. *J. Chem. Phys.* **2013**, 139, 164305.
- (7) Biondini, F.; Brunetti, B. G.; Candori, P.; De Angelis, F.; Falcinelli, S.; Tarantelli, F.; Moix Teixidor, M.; Pirani, F.; Vecchiocattivi, F. Penning ionization of N_2O molecules by He^* . *J. Chem. Phys.* **2005**, 122, 164307.
- (8) Ben Arfa, M.; Lescop, B.; Cherid, M.; Brunetti, B.; Candori, P.; Malfatti, D.; Falcinelli, S.; Vecchiocattivi, F. Ionization of ammonia molecules by collision with metastable neon atoms. *Chem. Phys. Lett.* **1999**, 308, 71–77.
- (9) Olney, T. N.; Cooper, G.; Chan, W. F.; Burton, R. G.; Brion, C. E.; Tan, K. H. Quantitative studies of the photoabsorption, photoionization, and ionic photofragmentation of methyl fluoride at VUV and soft X-ray energies (7–250 eV) using dipole electron scattering and synchrotron radiation. *Chem. Phys.* **1994**, 189, 733–756.
- (10) Brunetti, B.; Candori, P.; De Andres, J.; Pirani, F.; Rosi, M.; Falcinelli, S.; Vecchiocattivi, F. Dissociative Ionization of Methyl Chloride and Methyl Bromide by Collision with Metastable Neon Atoms. *J. Phys. Chem. A* **1997**, 101, 7505–7512.

- (11) Bertsche, B.; Jachymski, K.; Jankunas, J.; Hapka, M.; Idziaszek, Z.; Osterwalder, A. Temperature Insensitive Stereodynamics of the $\text{Ne}(3\text{P}_2) + \text{ND}_3$ Reaction Below 1 K. **2014**, submitted.
- (12) Bertsche, B.; Jankunas, J.; Osterwalder, A. Low temperature collisions between neutral molecules in merged molecular beams. *Chimia* **2014**, in press.
- (13) Jankunas, J.; Bertsche, B.; Jachymski, K.; Hapka, M.; Osterwalder, A. Dynamics of gas phase $\text{Ne}^* + \text{NH}_3$ and $\text{Ne}^* + \text{ND}_3$ Penning ionisation at low temperatures. in preparation.
- (14) Henson, A. B.; Gersten, S.; Shagam, Y.; Narevicius, J.; Narevicius, E. Observation of Resonances in Penning Ionization Reactions at Sub-Kelvin Temperatures in Merged Beams. *Science* **2012**, 338, 234–237.
- (15) Lavert-Ofir, E.; Shagam, Y.; Henson, A. B.; Gersten, S.; Kłos, J.; Żuchowski, P. S.; Narevicius, J.; Narevicius, E. Observation of the isotope effect in sub-kelvin reactions. *Nat. Chem.* **2014**, 6, 332–335.
- (16) Rangwala, S. A.; Junglen, T.; Rieger, T.; Pinkse, P. W. H.; Rempe, G. Continuous source of translationally cold dipolar molecules. *Phys. Rev. A* **2003**, 67, 043406.
- (17) Sommer, C.; Van Buuren, L. D.; Motsch, M.; Pohle, S.; Bayerl, J.; Pinkse, P. W. H.; Rempe, G. Continuous guided beams of slow and internally cold polar molecules. *Faraday Discuss* **2009**, 142, 203.
- (18) Bertsche, B.; Osterwalder, A. Dynamics of individual rotational states in an electrostatic guide for neutral molecules. *Phys. Chem. Chem. Phys.* **2011**, 13, 18954.
- (19) Shagam, Y.; Narevicius, E. Sub-Kelvin Collision Temperatures in Merged Neutral Beams by Correlation in Phase-Space. *J. Phys. Chem. C* **2013**, 117, 22454–22461.
- (20) Lane, I. C.; Powis, I. Changeable Behavior in the Unimolecular Decay Channels of Electronically Excited States of CH_3B^+ and CH_3Cl^+ . *J. Phys. Chem.* **1993**, 97, 5803–5808.

- (21) Eland, J. H. D.; Frey, R.; Kuestler, A.; Schulte, H.; Brehm, B. Unimolecular Dissociations and Internal Conversions of Methyl Halide Ions. *Int. J. Mass Spec. Ion. Phys.* **1976**, 22, 155–170.
- (22) de Miranda, M. H. G.; Chotia, A.; Neyenhuis, B.; Wang, D.; Quémener, G.; Ospelkaus, S.; Bohn, J. L.; Ye, J.; Jin, D. S. Controlling the quantum stereodynamics of ultracold bimolecular reactions. *Nat. Phys.* **2011**, 7, 502–507.